A High-Bandwidth Electrical-Waveform Generator Based on Aperture-Coupled Striplines for OMEGA Pulse-Shaping Applications

Pulsed-laser systems emit optical pulses having a temporal pulse shape characteristic of the particular type of laser design. Advances in technology have produced laser-pulse-shaping systems where the laser temporal profile can be specified in advance and controlled to a high degree of accuracy.[1–3] A pulse-shaping system has been in operation on OMEGA for several years. Temporally shaped optical pulses can be produced by applying shaped electrical waveforms to a dual-channel integrated-optics modulator.[1–3] These shaped electrical waveforms are sent to the optical modulator synchronized with the passage through the modulator of an optical pulse from a single-longitudinal-mode (SLM) laser.[4] The optical pulse exiting the modulator is then shaped in accordance with the voltage-dependent transfer function of the modulator. Hence, the electrical-waveform generator is an important component in any optical-pulse-shaping system incorporating optical modulators. This article discusses a greatly simplified pulse-shaping system based on an aperture-coupled-stripline (ACSL) electrical-waveform generator under development for OMEGA, and compares its many advantages over the existing OMEGA pulse-shaping system.

The Present OMEGA Pulse-Shaping System

The OMEGA pulse-shaping system uses an electrical-waveform generator based on an electrical reflection from a variable-impedance microstrip line (VIMSL).[3] Electrical-waveform generators based on stripline technology offer the highest temporal resolution over other systems due to their high-bandwidth capabilities, stripline-fabrication procedures, and achievable tolerances. The present OMEGA pulse-shaping system (outlined in Fig. 73.1) consists of many components. A cw mode-locked (CWML) laser is used to seed a regenerative amplifier (regen). The temporal width of the optical pulse injected into this regen is stretched in time with an intracavity etalon.[5] The output of the regenerative amplifier is amplified, and its leading edge is steepened with a stimulated Brillouin scattering (SBS) reflection from CCL_4.[6] This SBS pulse is amplified and sent to a fiber distribution system to illuminate photoconductive (PC) switches. Illumination of the PC switches activates the electrical-waveform generator, which produces the temporally shaped electrical waveforms that are sent to the optical modulator.[3,7] The subsequently shaped optical pulse from the modulator is sent to the OMEGA
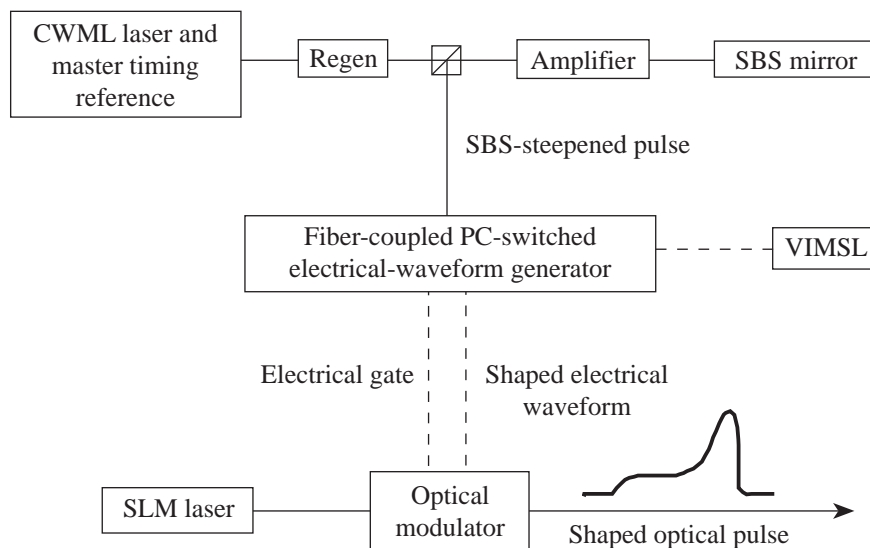

Figure 73.1
The OMEGA optical-pulse-shaping system. A cw mode-locked (CWML) laser seeds a regenerative amplifier (regen) whose output pulse is amplified and steepened by a stimulated Brillouin scattering (SBS) mirror. The SBS pulse activates a photoconductively (PC) switched electrical-waveform generator that drives the two channels of an optical modulator. The output from a single-longitudinal-mode (SLM) laser is temporally shaped by the optical modulator and injected into the OMEGA laser.

E8890

amplifiers with timing referenced with respect to the activation of the PC switches by the SBS pulse.

The VIMSL in OMEGA's electrical-waveform generator is a two-port electrical device.[3,7] A square electrical pulse is sent into one port of the device and propagates to the second terminated port. A shaped electrical waveform, generated by reflections along the length of the VIMSL, exits from the VIMSL through the input port and is sent to the optical modulator. This electrical-waveform generator has some anomalies that must be mitigated to achieve a high contrast (i.e., the ratio of the maximum pulse amplitude to the prepulse noise). The square electrical waveform sent to the VIMSL has a voltage stair step that is attributable to the finite "off" impedance and nonzero "on" impedance of the PC switches. The effects of this dc step are substantially minimized by applying a temporal delay to the shaped electrical waveform. In addition, there is a capacitively coupled voltage spike on the voltage waveform applied to the modulator that is attributable to the capacitance of the PC switch in the off state. To eliminate this prepulse and improve the contrast of the shaped optical pulses, a square electrical gate pulse is applied to the second channel of the modulator.

The ACSL Pulse-Shaping System

A pulse-shaping system with an electrical-waveform generator based on an ACSL has been developed. A layout of this ACSL pulse-shaping system is shown in Fig. 73.2. A square electrical waveform from a commercially available pulse generator is sent to an ACSL. The ACSL generates a shaped electrical waveform that is sent directly to the optical modulator for pulse shaping.

The design of the electrical-waveform generator is based on a four-layer, four-port ACSL and is modeled as a four-port electrical directional coupler. An exploded view of a practical device with four layers of material having dielectric constant ε_r is shown in Fig. 73.3. The important region of the ACSL for pulse shaping is the coupling region shown in cross section in Fig. 73.4. In operation, a square electrical waveform is launched into port 1 and propagates along electrode 1 to the terminated port 2 of the ACSL. As the square electrical waveform propagates along electrode 1 in the coupling region, the electrical signal is coupled through an aperture to electrode 2 in the backward direction and exits at port 4. By properly varying the width of the coupling aperture (s in Fig. 73.4) along the length of the ACSL, any desired temporally shaped electrical waveform can be generated at port 4 and sent to optical modulators for pulse shaping.

The ACSL system is characterized by an input and output impedance. The characteristic impedance Z_0 of the system is chosen to be 50 Ω to match the input impedance of the modulator channels. Ports 2 and 3 of the ACSL are terminated with this characteristic impedance to prevent reflections at these ports. The transition section of the ACSL is designed to accommodate the electrical connectors (stripline end launchers) required to transmit electrical signals from the standard coaxial electrical cables used as input and output to the ACSL to the coupling region of the ACSL (illustrated by the cross-sectional geometry in Fig 73.4). In the transition region (and in the coupling region when the aperture width is zero), the system can be thought of as two separate uncoupled and noninteracting ordinary striplines. To achieve a 50-Ω stripline in this section, the width of the electrode w is determined from well-known relations[8] involving the material parameters and the geometry of the ACSL.

To design and produce shaped voltage waveforms at port 4 of an ACSL, the electrical coupling coefficient from electrode 1 to electrode 2 (i.e., the ratio of the output-pulse voltage at port 4 to the input-pulse voltage at port 1) as a function of
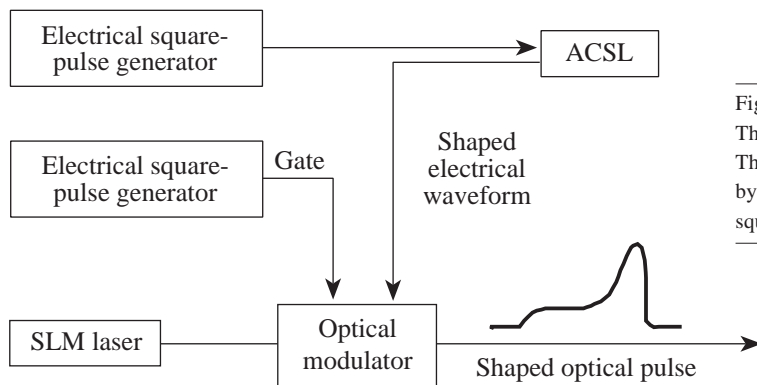

Figure 73.2
The aperture-coupled-stripline (ACSL) optical-pulse-shaping system. The output from an electrical square-pulse generator is temporally shaped by an ACSL and used to drive an optical modulator. A separate electrical square-pulse generator is used to gate the second channel of the modulator.
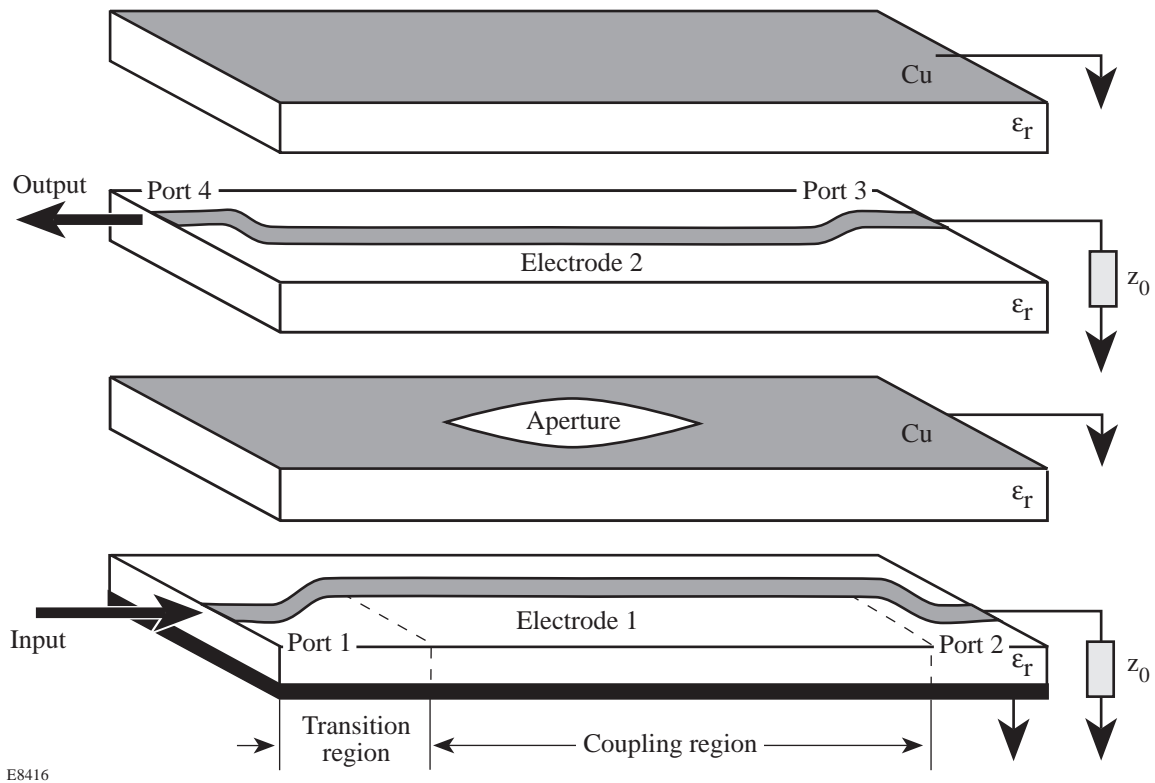
E8891

E8416

Figure 73.3
Exploded view of a practical four-layer, four-port ACSL. A square electrical waveform is launched into port 1 and propagates along electrode 1 to the terminated port 2. The electrical signal is coupled through an aperture to electrode 2 in the backward direction and a shaped electrical waveform exits at port 4.

aperture width s must be known. It is difficult to calculate this explicitly; however, simple experiments have been performed to measure this dependence. The data from these measurements are used in our model for designing ACSL devices.
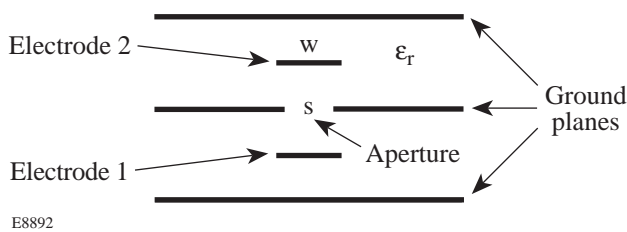

E8892

Figure 73.4
Cross-sectional view of an ACSL in the coupling region of Fig. 73.3. The electrode width w is chosen to provide a 50-Ω impedance structure. The amount of electrical coupling from electrode 1 to electrode 2 depends on the aperture width s.

Several ACSL devices have been fabricated and tested to determine the dependence of the electrical coupling coefficient on the aperture width s. A typical structure consists of four layers of RT/duroid[®9] 5880 microwave laminate material ($\varepsilon_r = 2.2$) sandwiched together as illustrated in Fig. 73.3. The two outer layers are 0.125 in. thick with 1 oz/ft^2 of copper on their outer surfaces. The stripline electrode width (w in Fig. 73.4) on the opposite side of these layers is 0.075 in. (experimentally verified to provide a 50-Ω impedance) and is machined with a precision programmable milling machine. (Note that electrode 2 in Fig. 73.3 is shown on an intermediate layer. This is for illustration purposes only. This electrode in our device is machined on the bottom of the layer above it, making the two outer layers completely identical.) The two center layers are 0.031 in. thick. One center layer has no copper on either surface and is used as a dielectric spacer. The other center layer has 1 oz/ft^2 of copper on one side only, with copper removed to form the appropriate coupling aperture. The

structure is easily disassembled to replace the aperture layer to produce different shaped electrical waveforms. Several other ACSL geometries with different layer thickness and electrode widths were tested, but as will be shown below, the above geometry produces a sufficiently high electrical coupling coefficient for our pulse-shaping application.

Three apertures having a width *s* that varies along the length of the line with the functional form of a simple Gaussian are used in the above structure to determine the dependence of the electrical coupling coefficient on the aperture width *s*. The maximum aperture widths of the three Gaussians are 5, 10, and 20 mm. Voltage measurements are made with a high-bandwidth (20-GHz)[10] sampling oscilloscope equipped with an electrical square-pulse generator for time domain reflectometer (TDR) measurements. The pulse from the TDR channel is sent into port 1 of the ACSL, and the output from port 4 is measured with a separate, high-bandwidth (20-GHz) channel of the oscilloscope. The time axis of the measured voltage waveforms is mapped to position along the ACSL using the electrical propagation velocity in the RT/duroid® material. From our measurements on the three Gaussian apertures, the electrical coupling coefficient versus aperture width is obtained and shown in Fig. 73.5. The data in Fig. 73.5 are used in our model to design ACSL devices that produce specific voltage waveforms for the optical-pulse-shaping system.
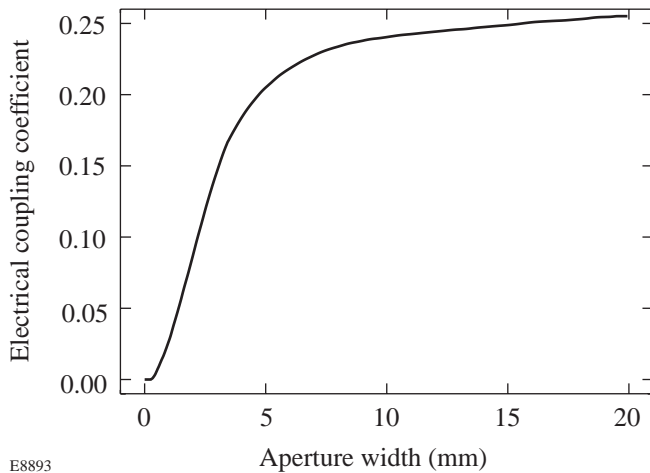

E8893

Figure 73.5
The electrical coupling coefficient, defined as the ratio of the output voltage at port 4 to the input voltage at port 1 in Fig. 73.3, plotted as a function of aperture width for an ACSL with the geometry discussed in the text.

The output voltage measured at port 4 of an ACSL with 5-mm-Gaussian aperture is plotted with a solid line in Fig. 73.6 (normalized to the voltage of the input square pulse

applied to port 1) along with the prediction of our model plotted with a dashed line. For high coupling coefficients, depletion of the input square-pulse voltage as it propagates along electrode 1 cannot be neglected and is included in our model.
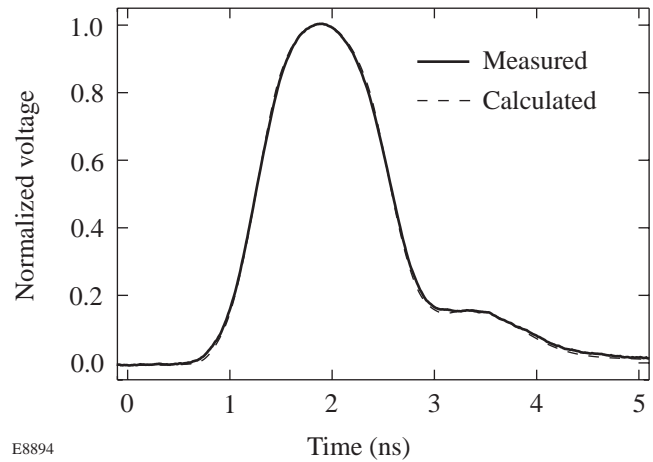

E8894

Figure 73.6
The measured output voltage waveform (solid line) from an ACSL having a Gaussian aperture along the length of the coupling region with a 5-mm maximum aperture width. The calculated output voltage from this structure (dashed line) is also shown.

Temporally shaped optical pulses have been produced using the pulse-shaping system shown in Fig. 73.2 with the ACSL geometry described above. A commercially available square-pulse generator[11] that provides a 35-V square pulse with 100-ps rise time is used as input to the ACSL. The half-wave voltage of the optical modulators used for pulse shaping is approximately 8 V. Hence, the coupling coefficients of 0.25 (shown in Fig. 73.5) obtainable with the ACSL structure described above are adequate for this application. To verify our ACSL model, the output voltage at port 4 of an ACSL designed to produce a specific optical pulse shape is sent to an optical modulator. The measured shaped optical pulse from the modulator is plotted with a solid line in Fig. 73.7; the optical pulse shape that is desired from this system is plotted with a dashed line. This figure illustrates the excellent performance and predictability of the ACSL pulse-shaping system.

Pulse-Shaping-Systems Comparison
By comparing the pulse-shaping systems shown in Figs. 73.1 and 73.2, it can be seen that the ACSL system eliminates the need for the CWML laser, the regen with SBS pulse steepener and amplifier, the fiber distribution system, and the PC switches. The key operational advantage of the ACSL pulse-shaping system that allows this simplification is
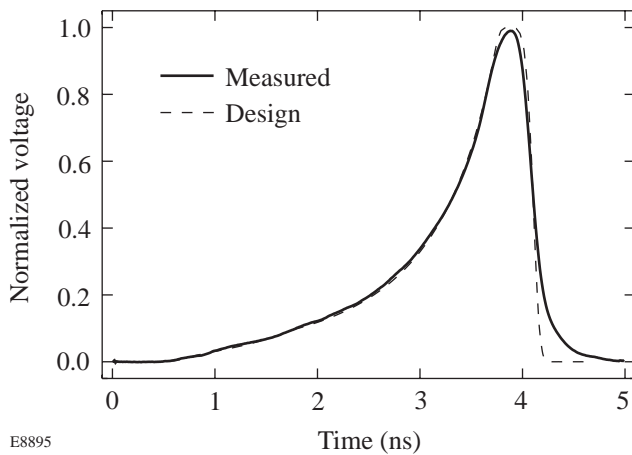
Figure 73.7
The measured temporally shaped optical pulse from an ACSL pulse-shaping system (solid line). The desired optical pulse shape (dashed line) from this system is also shown.

that the shaped electrical waveform from the ACSL exits from a different port than that used to input the square electrical pulse. Consequently, any suitable electrical square-pulse generator can be used to generate shaped electrical waveforms. In addition to this enormous simplification, there is no source of prepulse noise (capacitive voltage spike or dc offset voltage) since coupling cannot occur before application of the square electrical pulse to the ACSL. The system can also be accurately timed to the OMEGA master timing reference (38-MHz rf or 76-MHz CWML-laser optical pulses). The rms timing jitter between the 76-MHz CWML-laser optical pulses and the generation of the shaped electrical waveforms is measured to be less than 10 ps.

Conclusions

An optical-pulse-shaping system based on an ACSL has been designed and tested. This system produces temporally shaped optical pulses with high bandwidth suitable for OMEGA pulse-shaping applications. The design is a significant simplification over existing technology with improved performance capabilities.

REFERENCES

1. R. B. Wilcox, U.S. Patent No. 4,667,161 (19 May 1987).

2. R. B. Wilcox *et al.*, in *Laser Coherence Control: Technology and Applications*, edited by H. T. Powell and T. J. Kessler (SPIE, Bellingham, WA, 1993), Vol. 1870, pp. 53–63.

3. A. Okishev, M. D. Skeldon, S. A. Letzring, W. R. Donaldson, A. Babushkin, and W. Seka, in *Superintense Laser Fields*, edited by A. A. Andreev and V. M. Gordienko (SPIE, Bellingham, WA, 1996), Vol. 2770, pp. 10–17.

4. A. V. Okishev and W. Seka, IEEE J. Sel. Top. Quantum Electron. **3**, 59 (1997).

5. M. D. Skeldon and S. T. Bui, J. Opt. Soc. Am. B **10**, 677 (1993).

6. M. D. Skeldon, A. Okishev, A. Babushkin, and W. Seka, in *First Annual International Conference on Solid State Lasers for Application to Inertial Confinement Fusion*, edited by M. André and H. T. Powell (SPIE, Bellingham, WA, 1995), Vol. 2633, pp. 422–429.

7. M. D. Skeldon, A. Okishev, S. A. Letzring, W. R. Donaldson, K. Green, W. Seka, and L. Fuller, in *Optically Activated Switching IV*, edited by W. R. Donaldson (SPIE, Bellingham, WA, 1994), Vol. 2343, pp. 94–98.

8. B. C. Wadell, *Transmission Line Design Handbook* (Artech House, Boston, 1991).

9. RT/duroid®, Rogers Corporation, Microwave Division, Chandler, AZ 85226.

10. 20-GHz sampling oscilloscope, Model No. HP54120B/54124A, Hewlett Packard, Santa Clara, CA 95052-8059.

11. Pulse generator, Model No. 4500E, Picosecond Pulse Labs, Boulder, CO 80306.